THERMAL ASPECTS OF BEAM INTERCEPTING DIAGNOSTIC DEVICES

P. Strehl, GSI, Darmstadt, Germany

Abstract

Shown are the dependencies of thermal heating on the thermal characteristics of the stopping material and on the penetration depth of the particles considering DC-beams as well as intense pulsed beams up to some Megawatts pulse power. The results of relevant calculations based on solutions of the related partial differential equations of heat transfer are given for some typical projectile – target combinations. An example concerning beam loss in the beam pipe is given, too.

1 INTRODUCTION

Typical diagnostic devices which require the estimation of thermal effects are beam stoppers, slit systems, scrapers, wire scanners, profile grids, thin targets, septa. Since thermal effects in materials depend on the duty factor of the beam and the penetration depth of the impinging particles a classification distinguishing between DC-beams and intense pulsed beams has been proved to be useful. In both cases one has also to distinguish between $\mathbf{pd} \ll \mathbf{sd}$, $\mathbf{pd} \lesssim \mathbf{sd}$, $\mathbf{pd} > \mathbf{sd}$ with $\mathbf{pd}$ as the penetration depth of the impinging particles and $\mathbf{sd}$ as the longitudinal stopper dimension.

2 DC-BEAMS

For DC-beams and beams with a high duty cycle one has to consider the stationary temperature distribution $T(x, y, z)$ given by the solution of

$$\Delta T(x, y, z) = -\frac{1}{\lambda} \cdot \frac{\dot{Q}(x, y, z)}{V}\,, \qquad (1)$$

where λ $[\mathrm{W/mm \cdot K}]$ is the specific heat conductivity and $\frac{\dot{Q}}{V}$ $\left[\mathrm{W/mm^3}\right]$ is the heat deposited in the volume element V. Considering cylindrical symmetries and applying the method of finite differences the temperatures at the nodes of the mesh can be determined by iterating the equation

$$\begin{aligned} 0 \;=\; & C_I^+ \cdot T_{I+1,J} + C_I^- \cdot T_{I-1,J} + C_J^+ \cdot T_{I,J+1} \\ & + C_J^- \cdot T_{I,J-1} - A_{I,J} \cdot T_{I,J} + \dot{Q}_V(I,J) \end{aligned} \qquad (2)$$

where the C are determined by the structure of the mesh and the λ-*value*. The index I stands for the axial coordinate (z) and J for the radial coordinate (r). In case of $\mathbf{pd} \ll \mathbf{sd}$ $\dot{Q}_V(I,J)$ can be assumed zero and the deposited heat results from the boundary condition given by

$$T_{I=0,J} = T_{I=1,J} + \dot{Q}^*(J), \qquad (3)$$

where $\dot{Q}^*(J)$ is determined by $\frac{\dot{Q}}{F} = -\lambda \cdot \nabla T$ to $\dot{Q}^*(j) = \Delta z_1 \cdot \frac{\dot{Q}(r)}{F \cdot \lambda}$, with $\frac{\dot{Q}(r)}{F}$ $\left[\mathrm{W/mm^2}\right]$ as the radial power density of the beam. Δz_1 is the width of the mesh in axial direction and should be approximately pd. Figure 1 shows a calculated temperature distribution for $10\,\mathrm{MeV/u}$ Uranium ions stopped in Copper. Cooling was applied to the back plane ($T_{I_{\max},J} = 0$) and the shell ($T_{I,J_{\max}} = 0$) of the cylindrical Copper block.

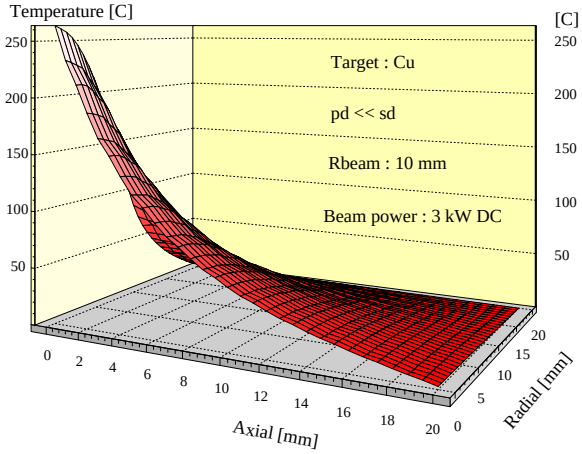

Figure 1: $10\,\mathrm{MeV/u}$ Uranium ions $\longrightarrow$ Cu

In addition to the maximum temperature $T_{\max}$ which in case of $\mathbf{pd} \ll \mathbf{sd}$ occurs at $z = 0$ and which is deciding for melting of the material the maximum power flow through the cooled surfaces has to be considered, too. This can be determined from

$$\begin{aligned} \frac{\dot{Q}(J)}{F} &= \lambda \cdot \frac{T_{I_{\max}-1,J} - T_{I_{\max},J}}{\Delta z}\,, \\ \frac{\dot{Q}(I)}{F} &= \lambda \cdot \frac{T_{I,J_{\max}-1} - T_{I,J_{\max}}}{\Delta r}, \end{aligned} \qquad (4)$$

which simplifies with $T_{I_{\max},J} = 0$ and $T_{I,J_{\max}} = 0$ due to cooling. For laminar water flow a mean power flow of about $120\,\mathrm{W/cm^2}$ [1] should not be exceeded to avoid film boiling. Obviously, the ratio of $T_{\max}$ and the maximum power flow depends on the λ-*value*, the beam radius, the length and the radius of the stoppingcylinder. To demonstrate the dependencies the table below gives $T_{\max}$ $[C]$, $\frac{\dot{Q}(J=0)}{F} = qz_{\max}$ and $\frac{\dot{Q}(I=0)}{F} = qr_{\max}$ in $\left[\mathrm{W/cm^2}\right]$ for the $10\,\mathrm{MeV/u}$ Uranium beam of Figure 1 stopped in Cu, Ta, W, Mo and Graphite (Gr).

U	$\rightarrow Gr$	$\rightarrow Cu$	$\rightarrow Mo$	$\rightarrow Ta$	$\rightarrow W$
T_{max}	1160	264	1191	1908	582
$\dot{q}r_{max}$	170	168	267	263	163
$\dot{q}z_{max}$	149	148	233	231	143

Although the penetration depth of 10 MeV protons in these materials is up to a factor of 4-7 larger than for Uranium $\mathbf{pd} \ll \mathbf{sd}$ still holds and, therefore the calculated values for T_{max}, $\frac{\dot{Q}(J=0)}{F} = qz_{\max}$ and $\frac{\dot{Q}(I=0)}{F} = qr_{\max}$ are nearly the same for all ions with the same beam parameters.

In case of larger energies ($\mathbf{pd} \lesssim \mathbf{sd}$) the $\dot{Q}_V(I,J)$ have to be calculated from energy loss tables [2] and inserted at the nodes of the mesh. Since the particles are stopped within the material the Bragg peak is reproduced in the $\dot{Q}_V(I,J)$ and, therefore $T_{\max}$ will not necessary occur at the front plane. This is demonstrated in Figure 2 for a beam of $100\,\mathrm{MeV/u}$ protons stopped in Copper, where the method of finite differences (FD) has been compared to the finite element method (FE) [3, 4].

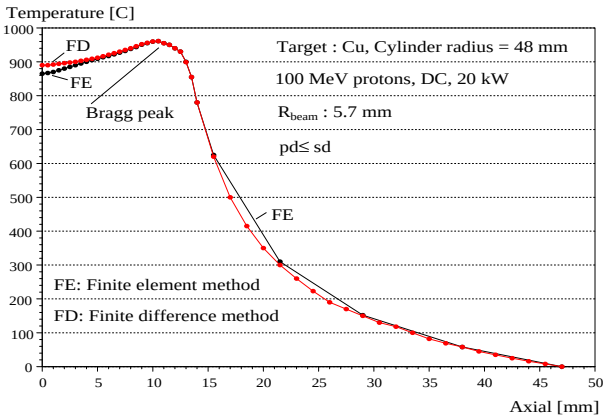

Figure 2: Comparison of FE and DE method

A further example in Figure 3 shows a 3-dimensional display for $1000\,\mathrm{MeV/u}$ Uranium ions stopped in Graphite. The next table gives the calculated T_{max}*-values* for the 5 materials.

U	$\rightarrow Gr$	$\rightarrow Cu$	$\rightarrow Mo$	$\rightarrow Ta$	$\rightarrow W$
T_{max}	538	305	946	3004	1022

3 INTENSE PULSED BEAMS

In case of $\mathbf{pd} \ll \mathbf{sd}$ cooling may not help if the deposited energy is sufficient to melt or even to vaporize the *range volume*, defined by $V(R_{beam}, pd) = \pi R_{beam}^2 \cdot pd$. Therefore, in a first estimation the beam energy of one beam pulse should be compared to the energy needed to melt the *range volume* (W_m).
Obviously, this estimation holds only if nearly no heat transfer to the material around the range volume takes place during the beam pulse length. To take the time dependence into account one has to solve the partial equation of heat transfer

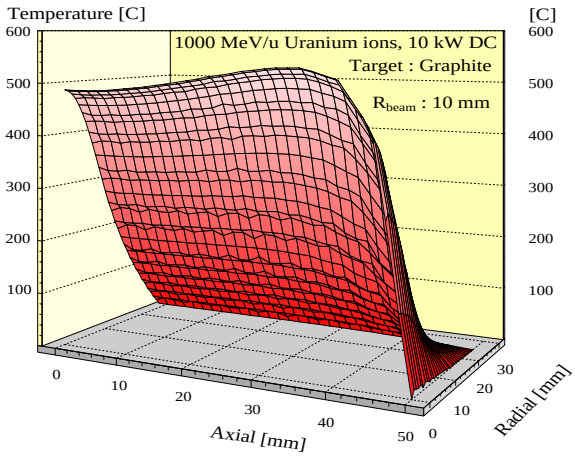

Figure 3: $1000\,\mathrm{MeV/u}$ Uranium ions $\longrightarrow$ Graphite

$$\frac{\partial T}{\partial t} = a^2 \cdot \Delta T(x,y,z) + \frac{\dot{Q}(x,y,z)}{V}\,, \qquad (5)$$

where $a^2 = \frac{\lambda}{c \cdot \rho}$ describes the time dependence of heat transfer. The next table gives the values of W_m and a^2 for the 5 materials.

	Gr	Cu	Mo	Ta	W	$Unit$
W_m	8	5.8	12	11	14.5	$[\mathrm{Ws/mm^3}]$
a^2	50	100	44	21	62	$[\mathrm{mm^2/s}]$

Figure 4 shows the distribution of temperatures for the selected materials along the beam axis after $1\,\mathrm{ms}$, assuming $pd = 0.1\,\mathrm{mm}$, a beam pulse length of $1\,\mathrm{ms}$ and a pulse power of $100\,\mathrm{kW}$.

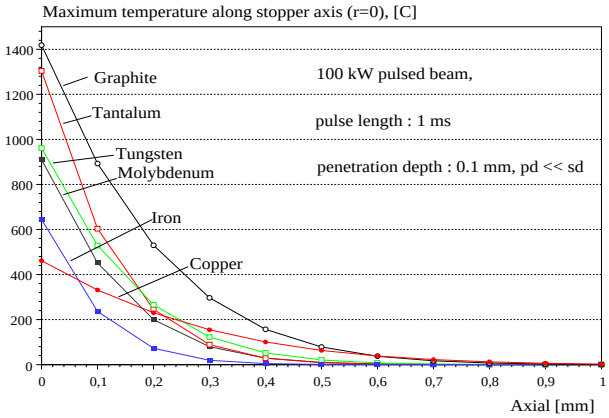

Figure 4: $100\,\mathrm{kW}$ pulsed beam stopped in various targets.

Another example is the design of a beam stopper which will be needed after the intensity upgrading of the Unilac. A $1.4\,\mathrm{MeV/u}$ Uranium beam of $1250\,\mathrm{kW}$ within $200\,\mu s$ has to be dumped. Since the penetration depth is only about $10\,\mu m$ the surface hit by the beam has to be enlarged by tilting the stopping plates. The design has been

optimized by using Equation 5 to calculate the temperature distribution in dependence of the enlarged beam radius for various materials. The calculated temperature distribution at the end of the beam pulse is shown in Figure 5 for a Tungsten plate. Although the calculation for Copper results in a $T_{\max}$ below the melting temperature the final design of the stopper will be made from Tungsten with a backing of Copper (see Figure 6) to avoid melting in case of beam misalignment or faults of focusing devices.

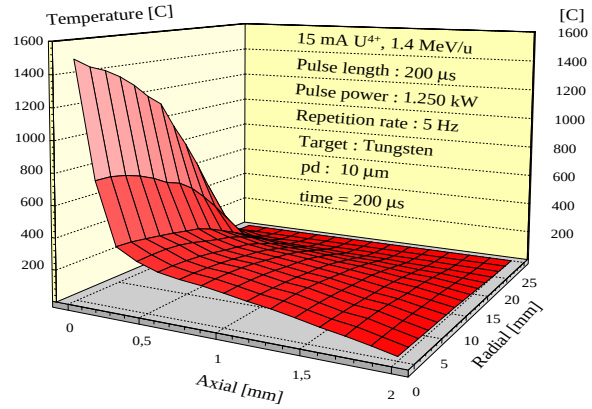

Figure 5: $1.4\,\mathrm{MeV/u}$ Uranium ions $\longrightarrow$ Tungsten

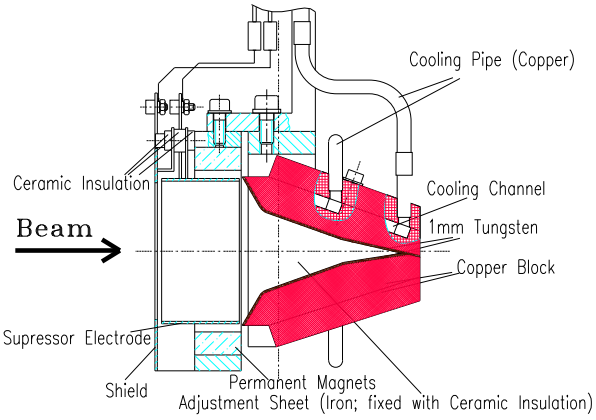

Figure 6: Beam stopper, parameter see Figure 5

In both examples above (Figure 4 and 5) the relation $\mathbf{pd} \ll \mathbf{sd}$ is fulfilled and therefore no Bragg peak occurs in the calculated temperature distributions. Due to the time dependence of heat transfer it is expected that in case $\mathbf{pd} \lesssim \mathbf{sd}$ and short intense beam pulses the Bragg peak will be reproduced more clearly in the temperature distribution as in the stationary case. This is demonstrated in Figure 7 for a $1000\,\mathrm{MeV/u}$ Uranium beam stopped in Graphite and should be compared to Figure 3.

In discussions about a heavy ion fusion facility the problem of tolerable beam losses has to be considered. Bi^{1+}-ions of $50\,\mathrm{MeV/u}$ are proposed as projectiles. Since $\mathrm{pd} \ll \mathrm{sd}$ holds the tolerable loss to avoid melting of the uncooled beam pipe is determined by the area hit by the

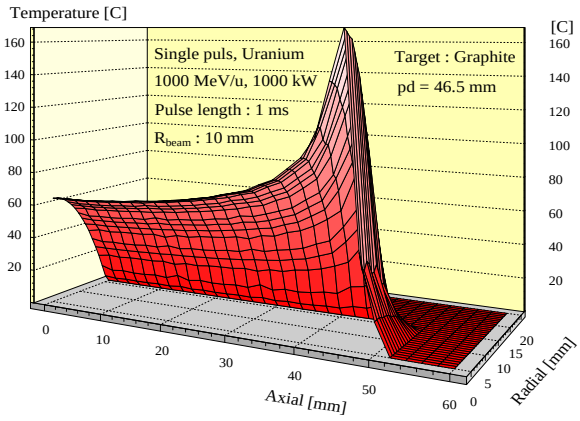

Figure 7: $1000\,\mathrm{MeV/u}$ Uranium ions $\longrightarrow$ Graphite

beam. Figure 8 shows $T_{\max}$ along the *z-axis* versus time.

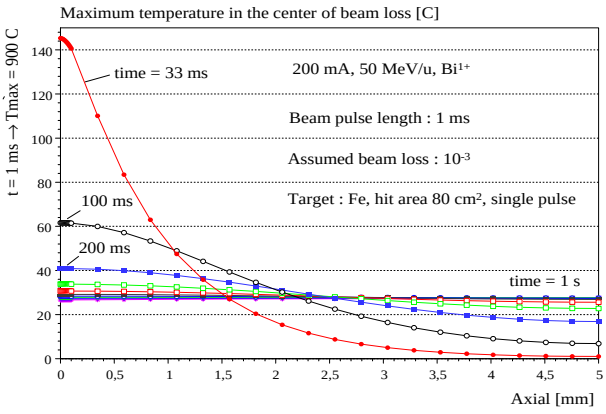

Figure 8: $T_{max}(z,t)$ in a beam pipe hit by the beam

Obviously, heating up of the beam pipe will depend on the repetition rate.

Conclusion: Due to the wide range of beam parameters and ion/target combinations only some selected topics thermal aspects have been discussed to describe the tools and to demonstrate the importance of the matter.

4 REFERENCES

[1] Gröber, Erk, Grigull, Die Grundgesetze der Wärmeübertragung, Springer-Verlag 1963.

[2] Ziegler, J. F., Handbook of stopping cross sections for energetic ions in all elements, Vol. 5, Pergamon Press 1980.

[3] Polivka, R. M., Wilson, E. L., Finite element analysis of nonlinear heat transfer problems, University of Berkeley, 1976.

[4] Riedel, C., Private communication, GSI-Darmstadt.